2008 American Control Conference
Westin Seattle Hotel, Seattle, Washington, USA
June 11-13, 2008

Simulation of Misfire and Strategies for Misfire Recovery of Gasoline HCCI

Karl Lukas Knierim, Sungbae Park {sungbae.park@us.bosch.com}, Jasim Ahmed, Aleksandar Kojic,
Research and Technology Center, Robert Bosch LLC, Palo Alto, CA, USA
Igor Orlandini, André Kulzer
Robert Bosch GmbH, Germany

***Abstract*— In HCCI mode with negative valve overlap, the understanding of the engine behavior in case of misfire and delayed combustion is important to provide a complete control strategy. A hybrid continuous zero dimensional model for gasoline HCCI, based on simplified chemical kinetics and a separate airflow model is introduced. CHEMKIN is used to simulate the chemical kinetics, whereas the airflow and the injection is simulated using MatLab. The model is compared to experimental data. The introduced model is used to analyze the effect of misfire and late combustions on the dynamics of the system. A state transition map is proposed to distinguish between misfire with and without recovery. Control strategies to improve the misfire recovery are suggested.**

I. INTRODUCTION

HCCI is an appealing combustion mode for gasoline engines. Efficiency increases of up to 30% compared to conventional spark ignited combustion and a significant reduction in NO_x emissions have been reported [1]. It involves a homogenized charge, which auto ignites due to the compression within the combustion stroke. It was first encountered by [2] as a combustion mode in two-stroke engines. It was used in a four stroke engine in [3]. In [4] first studies on the effects of the compression ratio and intake temperatures on HCCI combustion were shown. An overview of the potential and research in HCCI is given in [5]. Several strategies to achieve HCCI are known, among these intake manifold heating, external exhaust gas recirculation (EGR) and internal EGR. Internal EGR can be realized by either rebreathing strategies, which reopen the exhaust valve after the top dead center of gas exchange (TDCge) or by an early closing of the exhaust valve, also called negative valve overlap, to trap residual hot gas within the cylinder [6]. This paper describes HCCI using the negative valve overlap strategy. A lot of research on HCCI has been done during the last years [5]. Most of it focused on the emissions and the control of HCCI within its stable operating region. A multitude of simulation models have been developed for this purpose, ranging from complex CFD models [7] to zero-dimensional models [8], [9], [10].

The dynamics of HCCI, within its nominal operating region, under nominal conditions are well understood and control of HCCI at these points has been realized by various strategies in [11] [12] [13]. Still, it proves to be difficult to describe the dynamics of HCCI at the borders of the operating region, and to control HCCI effectively in case of misfires. This study focuses on developing a description of the behavior of HCCI in case of disturbance introduced misfire. Most of the current control oriented zero dimensional

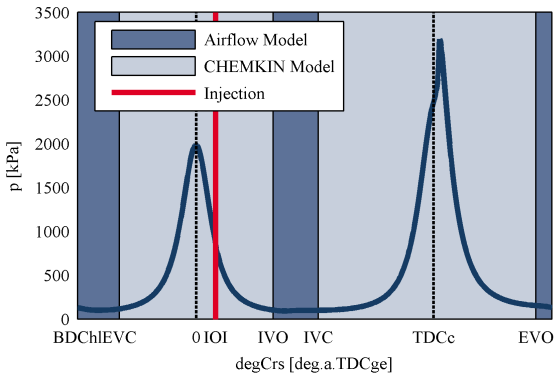

Fig. 1. Simulation using mixed Chemkin, airflow and injection model.

models [12] [9] use a prediction of the combustion phasing based on an Arrhenius or knock integral, and do not model explicitly the chemical kinetics of the combustion process. Therefore they can not capture the effect of partly burned fuel or misfires. To be able to model these phenomena, a continuous HCCI model using a simplified chemical mechanism for the oxidation of iso-octane (C_8H_{18}) and n-heptane (C_7H_{16}) coupled with an airflow model is introduced.

The model is used to simulate HCCI misfire dynamics. A disturbance is introduced into the HCCI cycle to delay the combustion phasing. The dynamic behavior of the system is observed during the following cycles. Based on the simulation results the behavior is divided into three different cases. The dynamics of HCCI are described as a state transition map and strategies to improve the recovery behavior of HCCI in case of misfire by closed loop control are outlined. A reasonable control input in each case can improve the recovery behavior as well as extend the region of recovery from misfire.

II. MODELING

In this section a model is introduced to investigate the dynamics of HCCI. To investigate misfire or delayed combustions it is necessary to use a model simulating chemical kinetics instead of using an Arrhenius or knock-integral based combustion prediction combined with an instantaneous heat release or a fixed burn rate [9],[12]. To achieve this, an already developed chemical reaction model [14] is coupled with an airflow and an injection model. The introduced model assumes that no reactions occur during the gas exchange phases and the injection takes place instantaneously, Figure 1. A Matlab simulation of the gas exchange process is used

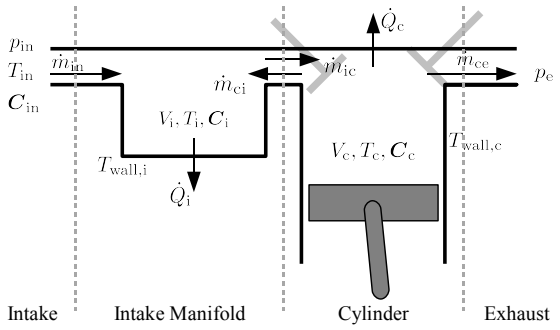

Fig. 2. Model setup, states and flows of the proposed model.

to simulate the airflow through open valves. The simulation output of the gas exchange process is used to initialize a CHEMKIN simulation of the reactions within the cylinder volume [15]. The injection is modeled as an instantaneous change of the in-cylinder state at the instant of injection IOI, interrupting the chemical reaction model.

A. Intake Manifold Model

In simulation a high back flow into the intake manifold in case of intermediate misfires has been observed, due to heat release during the trapping phase. Therefore, the intake manifold has been modeled as a space with a fixed volume to capture the effect of this back flow on the composition and temperature of the fresh charge in the next cycle. The intake manifold volume has as its state the concentrations of species and the mixture temperature. A visualization of the modeled spaces, conditions, states and flows is given in Figure 2.The intake manifold acts as a reservoir between the intake and the cylinder. The air flow between the intake and the intake manifold is modeled as $\dot{m}_{\text{in}}$ with the concentrations $\boldsymbol{C}_{\text{in}}$, and the temperature T_{in} similar to the modeled exhaust volume in [12]. The volume of the intake manifold is fixed at V_{i}, which gives the intake manifold pressure p_{i} using the ideal gas law,

$$p_{\text{i}} = R_u T_{\text{i}} \sum_i C_{\text{i},i}, \tag{1}$$

where $C_{\text{i},i}$ denotes the concentration of the i-th species inside of the intake manifold, R_u the universal gas constant, and T_{i} is the temperature of the gas inside of the intake manifold. The airflow $\dot{m}_{\text{in}}$ between the intake and the intake manifold with intake pressure p_{in} and intake temperature T_{in}, is now estimated by,

$$\dot{m}_{\text{in}} = f\left(p_{\text{i}}, p_{\text{in}}, T_{\text{in}}\right). \tag{2}$$

The steady state isentropic compressible flow is described in [16] and defines $f()$.

In case of an open intake valve the airflow between the cylinder and the intake manifold $\dot{m}_{\text{ic}}$ as well as the back flow $\dot{m}_{\text{ci}}$ is estimated by the same function

$$\dot{m}_{\text{ci}} = f\left(p_{\text{i}}, p_{\text{c}}, T_{\text{c}}\right) \qquad \dot{m}_{\text{ic}} = f\left(p_{\text{c}}, p_{\text{i}}, T_{\text{i}}\right), \tag{3}$$

where p_{c} denotes the current in-cylinder pressure, and T_{c} is the temperature inside the cylinder.

The mass fractions $\boldsymbol{Y}_j$ can be computed based on the concentrations $\boldsymbol{C}_{\text{j}}$, and the molar weights $\boldsymbol{M}_w$,

$$Y_{j,i} = \frac{C_{j,i} M_{w,i}}{\sum_i C_{j,i} M_{w,i}} \quad j := \{\text{in}, \text{i}, \text{c}\}, \tag{4}$$

where the index j denotes the intake, intake manifold, and cylinder.

Equations (2)-(3) yield the rate of change of the intake manifold concentrations $\dot{\boldsymbol{C}}_{\text{i}}$ as

$$\dot{C}_{\text{i},i} = \frac{\dot{m}_{\text{in}} Y_{\text{in},i} - \dot{m}_{\text{ic}} Y_{\text{i},i} + \dot{m}_{\text{ci}} Y_{\text{c},i}}{M_{w,i} V_{\text{i}}}. \tag{5}$$

The gas inside of the intake manifold is subjected to wall heat losses to the intake manifold wall. Assuming a simple wall heat loss model, this heat loss becomes

$$\dot{Q}_{\text{i}} = \lambda_{\text{i}} A_{\text{i}} \left(T_{\text{i}} - T_{\text{wall,i}}\right), \tag{6}$$

where λ_{i} denotes the heat transfer coefficient, A_{i} the wall area, and $T_{\text{wall,i}}$ is the wall temperature of the intake manifold.

Applying the first law of thermodynamics, the derivative of the intake manifold temperature w.r.t time becomes

$$\begin{aligned} \dot{T}_{\text{i}} = \frac{1}{\sum_i C_{\text{i},i} c_{\text{v},i}(T_{\text{i}})} \Bigg(& -\frac{\dot{Q}_{\text{i}}}{V_{\text{i}}} - \sum_i \dot{C}_{\text{i},i} h_i(T_{\text{i}}) \\ & + p_{\text{i}} \frac{\sum_i \dot{C}_{\text{i},i}}{\sum_i C_{\text{i},i}} + \dot{m}_{\text{in}} \frac{\sum_i Y_{\text{in},i} h_{\text{in},i}}{V_{\text{i}}} \\ & - \dot{m}_{\text{ic}} \frac{\sum_i Y_{\text{i},i} h_{\text{i},i}(T_{\text{i}})}{V_{\text{i}}} + \dot{m}_{\text{ci}} \frac{\sum_i Y_{\text{c},i} h_{\text{c},i}(T_{\text{c}})}{V_{\text{i}}} \Bigg). \end{aligned} \tag{7}$$

Equations (5) and (7) describe the dynamics of the intake manifold. The intake manifold model is run in parallel to both, the chemical kinetics model and the airflow model described in the following sections.

B. Chemical Kinetics Model

A simplified chemical kinetics model, describing the combustion of C_8H_{18} and C_7H_{16} has been developed by Orlandini et. al. and implemented into Chemkin. The chemical reactions are modeled using 31 different species, the different reactions and reaction coefficients are included in [14]. It has been successfully used within a multi zone model for the prediction of the combustion phasing. The chemical kinetics model can not handle mass flow in or out of the cylinder. Therefore it is run during the phases of the cycle where no mass flow occurs, Figure 1.

C. Airflow Model

The chemical kinetics model of the previous section does not model the mass flow into or from the cylinder. Therefore, a zero dimensional flow model based on the states inside of the cylinder, the intake manifold and the exhaust is used to describe the air exchange with the environment. The pressure inside of the cylinder, p_{c} can be expressed by the ideal gas law

$$p_{\text{c}} = R_u T_{\text{c}} \sum_i C_{\text{c},i}. \tag{8}$$

with $\boldsymbol{C}_\mathrm{c}$ being the concentration of species within the cylinder, T_c being the temperature of the in-cylinder gas. As in (2)-(3), the airflow between the cylinder and the exhaust manifold is described by $\dot{m}_\mathrm{ce} = f\left(p_\mathrm{e}, p_\mathrm{c}, T_\mathrm{c}\right)$. Using the mass fractions in (4), and the mass flows between the cylinder and the intake manifold (2)-(3), the time derivative of the concentrations inside of the cylinder $\dot{\boldsymbol{C}}_\mathrm{c}$ is given by

$$\dot{C}_{\mathrm{c},i} = \frac{\dot{m}_\mathrm{ic} Y_{\mathrm{i},i} - \dot{m}_\mathrm{ci} Y_{\mathrm{c},i} - \dot{m}_\mathrm{ce} Y_{\mathrm{c},i}}{M_{\mathrm{w},i} V_\mathrm{c}}. \tag{9}$$

The wall heat loss during the gas exchange is modeled by a Woshni heat loss model,

$$\dot{Q}_\mathrm{c} = h_w A_\mathrm{c} \left(T_\mathrm{c} - T_\mathrm{wall,c}\right), \tag{10}$$

where h_w is the Woshni heat loss coefficient [16], A_c describes the current cylinder wall area and $T_\mathrm{wall,c}$ is the wall temperature of the engine. Applying energy and mass balances for the in cylinder volume and accounting for the volumetric work output, the derivative of the in-cylinder temperature is similar to [8],

$$\begin{aligned}\dot{T}_\mathrm{c} = \frac{1}{\sum_i C_{\mathrm{i},i} c_{\mathrm{v},i}(T_\mathrm{i})} \Bigg(& -\frac{\dot{Q}_\mathrm{c}}{V_\mathrm{c}} - \sum_i \dot{C}_{\mathrm{c},i} h_c(T_\mathrm{c}) \\ & - \frac{\dot{V}_\mathrm{c}}{V_\mathrm{c}} \sum_i C_{\mathrm{c},i} h_{\mathrm{c},i}(T_\mathrm{c}) + p_\mathrm{c} \frac{\sum_i \dot{C}_{\mathrm{c},i}}{\sum_i C_{\mathrm{c},i}} \\ & - \left(\dot{m}_\mathrm{ci} + \dot{m}_\mathrm{ce}\right) \frac{\sum_i Y_{\mathrm{c},i} h_{\mathrm{c},i}(T_\mathrm{c})}{V_\mathrm{c}} \\ & + \dot{m}_\mathrm{ic} \frac{\sum_i Y_{\mathrm{i},i} h_{\mathrm{i},i}(T_\mathrm{i})}{V_\mathrm{c}} \Bigg). \end{aligned} \tag{11}$$

Combining (9) and (11) yields state equations of the in-cylinder dynamics during the gas exchange periods.

D. Injection Model

The injection of fuel into the cylinder is assumed to be instantaneous at the crank angle IOI. The desired amount of fuel m_inj is divided up into C_7H_{16} and C_8H_{18} in accordance to the assumed octane rating OCN

$$m_\mathrm{inj}^{C_8H_{18}} = \frac{\mathrm{OCN}}{100} m_\mathrm{inj} \qquad m_\mathrm{inj}^{C_7H_{16}} = m_\mathrm{inj} - m_\mathrm{inj}^{C_8H_{18}}$$

With the number of moles of the i-th species before the injection, N_i , the molar enthalpy of each species at the cylinder temperature at IOI, $\tilde{h}_{\mathrm{c},i}(T_\mathrm{c})$, the molar evaporation enthalpy of C_8H_{18} and C_7H_{16}, $\tilde{h}_\mathrm{evap}$, and the injection temperature T_inj, the internal energy after the injection of the fuel can be written as the sum of the internal energy before the injection and the amount of injected energy,

$$\begin{aligned} U = & \sum_i C_{\mathrm{c},i} \tilde{u}_{\mathrm{c},i}(T_\mathrm{c}) V_\mathrm{c} \\ & + \frac{m_\mathrm{inj}^{C_8H_{18}}}{M_{w,C_8H_{18}}} \left(\tilde{u}_{C_8H_{18}}(T_\mathrm{inj}) - \tilde{h}_\mathrm{evap}\right) \\ & + \frac{m_\mathrm{inj}^{C_7H_{16}}}{M_{w,C_7H_{16}}} \left(\tilde{u}_{C_7H_{16}}(T_\mathrm{inj}) - \tilde{h}_\mathrm{evap}\right), \end{aligned} \tag{12}$$

where $\tilde{u}_i(T)$ denotes the estimate of the internal molar energy of species i at temperature T. The internal energy

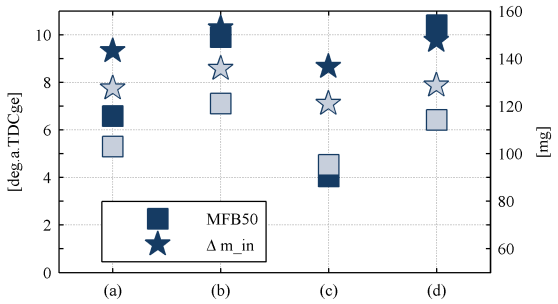

Fig. 3. Comparison between experimental steady state data (grey) and simulations (dark blue). EVO = 520deg.a.TDCge, EVC = 111.5deg.a.TDCge, IVO = 85deg.a.TDCge, IVC = 198deg.a.TDCge, m_inj = 6.91mg, IOI = 28.4deg.a.TDCge, OCN = 89, RPM = 2000. (a) ΔEVC = 0deg ΔIOI = 0deg; (b) ΔEVC = 3deg; (c) ΔEVC = $-$3deg; (d) ΔIOI = 15deg.

of the cylinder at a temperature $\bar{T}_\mathrm{c}$, with the composition $\bar{\boldsymbol{N}}_\mathrm{c}$ of the in cylinder species after the injection is

$$U(\bar{T}_\mathrm{c}) = \sum_i \tilde{u}_i(\bar{T}_\mathrm{c}) \bar{N}_{\mathrm{c},i}. \tag{13}$$

Applying the energy balance before and after the injection by combining (12) and (13) and solving for $\bar{T}_\mathrm{c}$ yields the temperature inside of the cylinder after the injection of fuel. Updating the concentrations vector completes the injection model.

E. Validation

The previously developed model will not be able to replicate a specific engine exactly due to the simplifications and drawbacks of a zero dimensional modeling approach. Although it would be possible to identify airflow and combustion parameters to improve the fit of the model to experimental data, a detailed identification was set aside for the moment. The model was compared to experimental data measured at a 4 cylinder research engine at the Robert Bosch Research Center, Schwieberdingen [17]. In Figure 3, experiments and simulations for three different EVC timings and a change in the injection timing, are plotted for the steady state cases. They are compared in terms of the combustion phasing, represented by angle at which 50% of the total heat is realeased, MFB50, and the intake air flow Δm_in. As can be seen, the model replicates the expected behavior of the system in a qualitative way. The airflow model predicts an airflow that is about 20mg too high, but is still showing the expected qualitative behavior. This results in an error of the prediction of MFB50 in the simulations. Nevertheless, the sytem behavior is comparable to the measurements. The direction of change of both parameters is correct for the input variation.

III. Misfire Simulation

Misfire in HCCI is sporadicly observed during steady state operation and encountered in case of load changes or switching operations between SI- and HCCI combustion. It is difficult to analyze misfire in experimental setups, therefore dynamic simulations are a good approach to analyze the dynamic behavior of misfire.

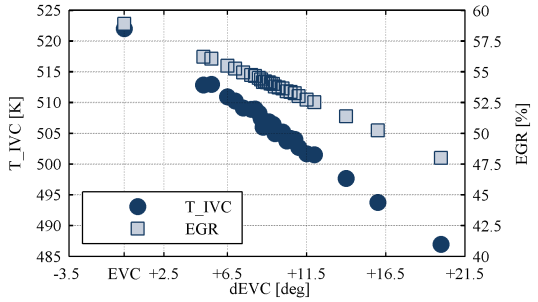

Fig. 4. Temperature at intake valve closing and EGR in the first cycle w.r.t. exhaust valve closing (EVC). RPM = 2000,T_{in} = 305K, p_{in} = 1bar, p_{in} = 1bar, p_e = 1bar, EVO = 540deg.a.TDCge, IVO = 85deg.a.TDCge,IVC = 195deg.a.TDCge, IOI = 28deg.a.TDCge, $m_{\text{inj}} = 6.9$mg, OCN = 89

Misfire and delayed combustion can for instance be caused by a lower temperature at intake valve closing T_{IVC}. A lower T_{IVC} can be provoked e.g. by a drop in temperature within the intake manifold, a disturbance in the airflow from the intake manifold, an error within the valve actuation, or a load or mode change. The intake manifold model introduced in Section II-A makes it impossible to instantaneously change the intake manifold temperature. Therefore a one cycle disturbance in EVC is introduced to affect the temperature at IVC.

The simulation is initiated at a steady state stable HCCI operating point, with a combustion phasing of MFB50 = 6.5deg.a.TDCc and an indicated mean effective pressure of the whole work cycle $\text{IMEP}_{\text{wc}} = 2.75$bar. By closing the exhaust valve later the amount of internal EGR is reduced and therefore the temperature T_{IVC} at intake valve closing decreases. The temperature at IVC and the resulting EGR are shown in Figure 4. Figure 5 illustrates the recovery and misfire behavior of the system. All simulations are started at the same initial in-cylinder gas temperature. Due to the delay in EVC the amount of trapped gas varies, and therefore the temperature at T_{IVC} is decreased. For smaller disturbances, this results in a delayed combustion (a), the temperature after the combustion is still in the same region as for the nominal case. For the simulation cases (b) and (c) the state of the mixture within the first cycle does not reach the necessary conditions for a complete combustion anymore. This results in a lower temperature at the end of the cycle. Within the trapping phase of the second cycle, the two cases split up. For some disturbances (b), the temperature within the trapping cycle is high enough to burn residual fuel during the recompression. In these cases, the injected fuel is burned directly after the injection. Although the temperature at the beginning of the high pressure phase is very high, there is no residual fuel or oxygen to result in a combustion within the combustion phase, nevertheless the temperature at the end of the second cycle is comparable to the gas temperature of a nominal combustion and will result in recovery during the following cycles. The third case (c) does not reach the conditions for the burning of fuel within the trapping cycle. Hence, the gas temperature decreases even further, and leads to a stalled engine. In Figure 6, the MFB50 of the first three consecutive cycles is shown w.r.t. T_{IVC} of the first cycle. As

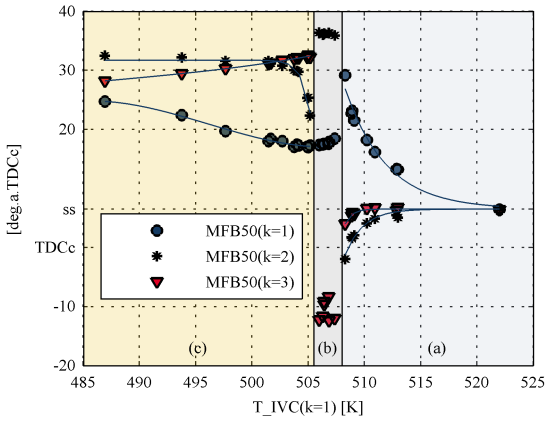

Fig. 6. MFB50 of the first to third cycle w.r.t. T_{IVC}.

already observed in Figure 5 the dynamic behavior of the model can be divided into three different cases:

- **(a)** the combustion is delayed by the decreased temperature. Due to the later combustion the wall heat loss is smaller. Hence, the temperature during the next cycle is higher than for the steady state case, the combustion in the second cycle occurs earlier than for the nominal case.
- **(b)** misfire occurs within the first cycle. Due to a combustion within the trapping cycle the engine recovers and shows a very early combustion in the third cycle.
- **(c)** misfire occurs within the first cycle, the engine does not recover and stalls due to the decreasing of the in-cylinder temperature.

Figure 6 illustrates the change of the dynamic behavior. As long as the disturbance is small enough the system remains within the region of attraction of nominal combustion (a). A too high disturbance pushes the system out of the region of the attraction of the nominal combustion and the model converges to another stable state without combustion (c). Of special interest is the case (b). Within the low pressure phase the residual fuel of the previous cycle burns and releases enough heat to enable the injected fuel to directly burn after the injection. Due to this combustion within the trapping cycle, the in-cylinder gas temperature is increased and work output is produced. The higher pressure within the cylinder leads to a back flow of hot burned gas into the cylinder manifold. The simulations predict a very early combustion within the third cycle. In Figure 7, it can be observed how case (a) and (b) converge to the nominal steady state combustion with MFB50 $\approx$ 6.5deg.a.TDCc and $\text{IMEP}_{\text{wc}} \approx 2.8$bar, whereas (c) shows only a very minor work output $\text{IMEP}_{\text{wc}} < 0.2$bar.

IV. Description of Misfire Behavior

The dynamics of HCCI, introduced by a disturbance of the temperature at intake valve closing can be divided into three different dynamics, depending on the magnitude of the disturbance. The HCCI combustion can be described by the state transition map in Figure 8. The states and transitions are explained in Table I. At each cycle the system moves alongside one of the transitions. Regarding to the size of the

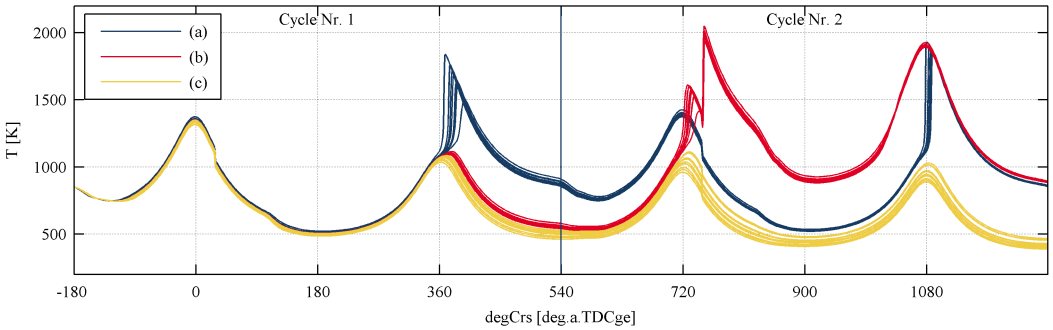

Fig. 5. Temperature traces for the first two cycles. Delay of EVC in the first cycle, second cycle with nominal EVC timing. (a) Delayed combustion, with full heat release during the first cycle, autonomous recovery in the second cycle. (b) Misfire during the first cycle, combustion of residual fuel during the compression in the trapping phase of the second cycle, temperature of residual gas is similar to (a) at the end of the second cycle. (c) Misfire in the first cycle, without recovery of gas temperature within the second cycle.

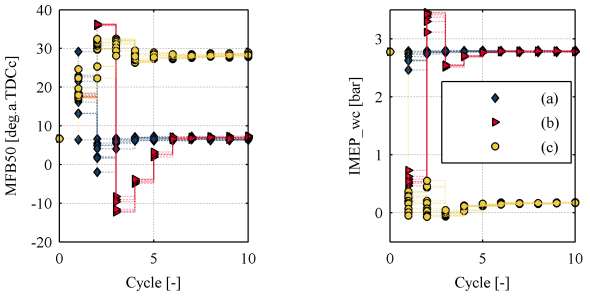

(a) MFB50 of 10 cycles. (b) IMEPwc of 10 cycles.

Fig. 7. Combustion features of the cycles after the disturbance.

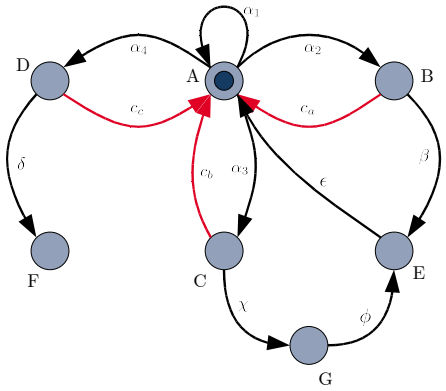

Fig. 8. State transition map, describing HCCI dynamics as the transition between states with the properties described in Table I.

disturbance the system is moved to either state B, C or D. Without any feedback control input the system would then follow its autonomous dynamic behavior:

- (a) $B \xrightarrow{\beta} E \xrightarrow{\epsilon} A$
- (b) $C \xrightarrow{\chi} G \xrightarrow{\phi} E \xrightarrow{\epsilon} A$
- (c) $D \xrightarrow{\delta} G$

V. Control of Misfire Dynamics

Most current control strategies for HCCI, [12],[18],[11] focus on the control of the dynamics described as case (a). In an idealized description they try to introduce the transition

TABLE I

States and Transitions of Figure 8

States

A	nominal steady state combustion
B	delayed combustion, with full heat release
C	misfire, with minor heat release
D	misfire, without heat release
E	advanced combustion
F	engine stalls
G	misfire during low pressure phase

Transitions

α_1	steady state combustion, no disturbance
α_2	minor disturbance, small decrease in T_{IVC} e.g. $T_{\text{IVC}} > 507$K
α_3	increased disturbance, higher impact on T_{IVC} e.g. $T_{\text{IVC}} > 505$K
α_4	T_{IVC} is below the threshold, no significant heat release during the high pressure phase, e.g. $T_{\text{IVC}} < 505$K
β	smaller wall heat loss results in higher temperature, resulting in advanced combustion
χ	combustion during trapping cycle, backflow into intake manifold, no combustion during trapping cycle
δ	temperature has dropped below the necessary temperature to initiate combustion
ϵ	autonomous recovery of HCCI combustion
ϕ	high temperature in third cycle results in advanced combustion

c_a in Figure 8 by feedback control. This involves usually a decrease of the EGR or a delay in the injection timing to prevent the advanced combustion within the second cycle. Applying the same strategy in case (b) or (c) is actually the opposite of the action necessary to bring the system back to stable combustion. Instead of decreasing the amount of EGR in these two cases it is necessary to increase the amount of EGR to keep more thermal energy inside of the cylinder. The following control inputs can improve the misfire recovery behavior and hereby describe the control inputs necessary to introduce the transitions c_a, c_b, and c_c:

- c_a a decrease in EGR or a delay in the injection timing to add a small delay to the combustion phasing to avoid the advanced combustion.
- c_b later injection to avoid full combustion during the

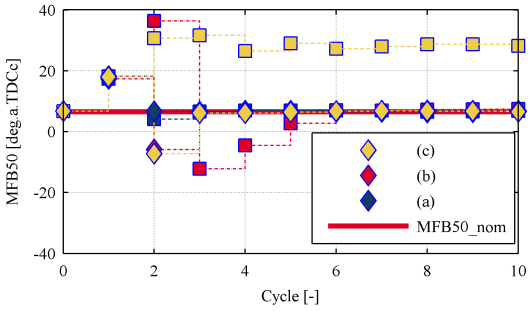

Fig. 9. Feedback control of examples for case (a), (b), and (c). Simulation of MFB50 without feedback (sqares) and with feedback input in second cycle (diamonds).

TABLE II

INPUT CORRECTION FOR STATE TRANSITION c_a, c_b, AND c_c

case	applied control offset
(a) $\Delta\text{EVC}(k=1) = 7\text{deg}$	$\Delta\text{EVC}(k=2) = 3\text{deg}$
(b) $\Delta\text{EVC}(k=1) = 8.75\text{deg}$	$\Delta\text{IVC}(k=2) = 70\text{deg}$ $\Delta m_{\text{inj}}(k=2) = -3.4\text{mg}$ $\Delta\text{IOI}(k=2) = 40\text{deg}$
(c) $\Delta\text{EVC}(k=1) = 11\text{deg}$	$\Delta\text{IVC}(k=2) = 70\text{deg}$ $\Delta\text{EVO}(k=2) = -30\text{deg}$ $\Delta\text{EVC}(k=2) = -30\text{deg}$ $\Delta m_{\text{inj}}(k=2) = -2.6\text{mg}$ $\Delta\text{IOI}(k=2) = 40\text{deg}$

trapping cycle, reduction in amount of injected fuel to account for residual fuel of the previous cycle.

- c_c earlier exhaust valve closing to trigger combustion of residual fuel within the trapping cycle, later injection and reduction of injected fuel to account for residual fuel of the previous cycle.

Examples for the three suggested control strategies are presented in Figure 9, with the necessary control inputs as noted in Table II. It can be observed in Figure 9 that the suggested inputs in fact improve the recovery behavior. In case (a), it is possible to design a feedback map, which gets the combustion phasing to the nominal value, within one cycle. In case (b), the phasing still becomes early within the second cycle, but due to the reduced injection amount, the temperature at the end of the second cycle is equal to the nominal case and the phasing reaches its nominal value during the third cycle. In case (c), the improvement is most obvious. Without feedback the engine would stall. The increased EGR makes combustion within the trapping cycle possible, and therefore the system recovers in a similar way to case (b). The nominal value is reached within the third cycle. The region of recovery from misfire can therefore be increased.

VI. CONCLUSIONS

The dynamics of HCCI misfire and recovery behavior have been analyzed. They can be divided into three different dynamical regions. The dynamics are described as a state transition map. By feedback control, new transitions can be introduced into the system. Applying different control inputs in each of the three dynamical regions improves the recovery behavior significantly and extends the robustness of the system against disturbances.

To apply the suggested control strategies it is necessary to distinguish between the three different types of delayed combustion. Distinguishing between case (b) and (c) will require additional information about the system. Observers of the thermodynamic state of the mixture within the cylinder are necessary to observe the temperature and other states in order to apply the correct control strategy.

ACKNOWLEDGMENTS

We thank Dr.-Ing. Jean-Pierre Hathout, Dr.-Ing. Roland Karrelmeyer, Dr.-Ing. Axel Löffler and Dr.-Ing. Wolfgang Fischer at Corporate Research, Robert Bosch GmbH, Germany, for measurements and suggestions.

REFERENCES

[1] H. Zhao, J. Li, T. Ma, and N. Ladommatos, "Performance and analysis of a 4-stroke multi-cylinder gasoline engine with cai combustion," SAE paper 2002-01-0420, 2002.

[2] S. Onish, S. H. Jo, K. Shoda, P. D. Jo, and S. Kato, "Active thermo-atmosphere combustion (atac) - a new combustion process for internal combustion engines," SAE paper 790501, 1979.

[3] P. M. Najt and D. E. Foster, "Compression-ignited homogeneous charge combustion," SAE paper 830264, 1983.

[4] R. H. Thring, "Homogeneous-charege compression ignition (hcci) engines," SAE paper 892068, 1989.

[5] K. Epping, S. Aceves, R. Bechtold, and J. Dec, "The potential of hcci combustion for high efficiency and low emissions," SAE paper 2002-01-1923, 2002.

[6] D. Law, J. Allen, D. Kemp, G. Kirkpatrick, and T. Copland, "Controlled combustion in an ic-engine with a fully variable valve train," SAE paper 2001-01-1030, 2001.

[7] S. C. Kong, C. D. Marriot, R. D. Reitz, and M. Christensen, "Modeling and experiments of hcci engine combustion using detailed chemical kinetics with multi-dimensional cfd," *Combustion Science and Technology*, vol. 27, pp. 31–43, 1981.

[8] G. M. Shaver, J. C. Gerdes, M. J. Roelle, P. A. Caton, and C. F. Edwards, "Dynamic modeling of residual-affected homogeneous charge compression ignition engines with variable valve actuation," *Journal of Dynamic Systems, Measurement, and Control*, vol. 127, pp. 374–381, 2005.

[9] D. J. Rausen, A. G. Stefanoupoulou, J.-M. Kang, J. A. Eng, and T.-W. Kuo, "A mean-value model for control of homogeneous charge compression ignition (hcci) engines," *ASME Journal of Dynamic Systems, Measurement and Control*, vol. 127, pp. 355–362, 2005.

[10] N. J. Killingsworth, S. M. Aceves, D. L. Flowers, and M. Kristić, "A simple hcci engine model for control," in *Procedings of the 2006 IEEE International Conference on Control Applications*, 2006, pp. 2424–2429.

[11] R. Karrelmeyer, J. Häring, W. Fischer, and J.-P. Hathout, "Closed-loop control of a 1-cylinder gasoline hcci-engine in dynamic operation," E-COSM - Rencontres Scientifiques de l'IFP 2006, 2006.

[12] G. M. Shaver, "Physically-based modeling and control of residual-affected hcci engines using variable valve actuation," Ph.D. dissertation, Stanford University, 2005.

[13] J. Bengtsson, P. Strandh, R. Johansson, P. Tunestal, and B. Johansson, "Model predictive control of homogeneous charge compression ignition (hcci) engine dynamics," in *Proceedings of the 2006 International Conference on Control Applications*, 2006.

[14] I. Orlandini, A. Kulzer, F. Weberbauer, and M. Rauscher, "Simulation of self ignition in hcci and partial hcci engines using a reduced order model," SAE paper 2005-01-0159, 2004.

[15] *CHEMKIN Software Theory Manual*, Reaction Design, 2006.

[16] J. B. Heywood, *Internal Combustion Engine Fundamentals*. McGraw-Hill Inc., 1988.

[17] A. Kulzer, J.-P. Hathout, C. Sauer, R. Karrelmeyer, W. Fischer, and A. Christ, "Multi-mode combustion strategies with cai for a gdi engine," SAE paper 2007-01-0214, 2007.

[18] J. Bengtsson, P. Strandh, R. Johansson, P. Tunestal, and B. Johansson, "Control of homogeneous charge compresseion ignition (hcci) engine dynamics," in *Proceeding of the 2004 American Control Conference*, 2004, pp. 4048–4053.